



## Application of Optical Reflex Sensors

### TCRT1000, TCRT5000, CNY70

Vishay Semiconductor optoelectronic sensors contain infrared-emitting diodes as a radiation source and phototransistors as detectors.

#### Typical applications include:

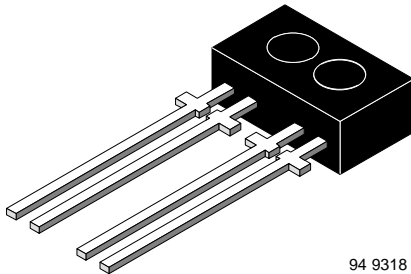
- Copying machines
- Video recorders
- Proximity switch
- Vending machines
- Printers
- Object counters
- Industrial control

#### Special features:

- Compact design
- Operation range 0 to 20 mm
- High sensitivity
- Low dark current
- Minimized crosstalk
- Ambient light protected
- Cut-off frequency up to 40 kHz
- High quality level, ISO 9000
- Automated high-volume production

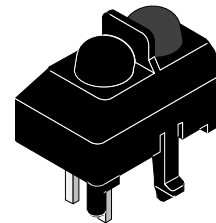
These sensors present the quality of perfected products. The components are based on Vishay Semiconductor's many years' experience as one of Europe's largest producers of optoelectronic components.

### Sensor Drawings



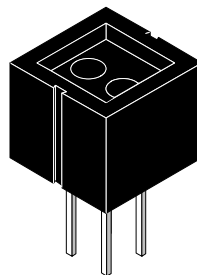
94 9318

**TCRT1000**



94 9442

**TCRT5000**



94 9320

**CNY70**



## Optoelectronic Sensors

In many applications, optoelectronic transmitters and receivers are used in pairs and linked together optically. Manufacturers fabricate them in suitable forms. They are available for a wide range of applications as ready-to-use components known as couplers, transmissive sensors (or interrupters), reflex couplers and reflex sensors. Increased automation in industry in particular has heightened the demand for these components and stimulated the development of new types.

### General Principles

The operating principles of reflex sensors are similar to those of transmissive sensors. Basically, the light emitted by the transmitter is influenced by an object or a medium on its way to the detector. The change in the light signal caused by the interaction with the object then produces a change in the electrical signal in the optoelectronic receiver.

The main difference between reflex couplers and transmissive sensors is in the relative position of the transmitter and detector with respect to each other. In the case of the transmissive sensor, the receiver is opposite the transmitter in the same optical axis, giving a direct light coupling between the two. In the case of the reflex sensor, the detector is positioned next to the transmitter, avoiding a direct light coupling.

The transmissive sensor is used in most applications for small distances and narrow objects. The reflex sensor, however, is used for a wide range of distances as well as for materials and objects of different shapes.

In the following chapters, we will deal with reflex sensors – placing particular emphasis on their practical use. The components TCRT1000, TCRT5000 and CNY70 are used as examples. However, references made to these components and their use apply to all sensors of a similar design.

The reflex sensors TCRT1000, TCRT5000 and CNY70 contain IR-emitting diodes as transmitters and phototransistors as receivers. The transmitters emit radiation of a wavelength of 950 nm. The spectral sensitivity of the phototransistors are optimized at this wavelength.

There are no focusing elements in the sensors described, though lenses are incorporated inside the TCRT5000 in both active parts (emitter and detector). The angular characteristics of both are divergent. This is necessary to realize a position-independent function for easy practical use with different reflecting objects.

In the case of TCRT5000, the concentration of the beam pattern to an angle of 16° for the emitter and 30° for the detector results in operation at an increased range with optimized resolution. The emitting and acceptance angles in the other reflex sensors are about 45°. This is an advantage in short distance operation.

The main difference between the sensor types is the mechanical outline (as shown in the figures, see previous page ), resulting in various electrical parameters and optical properties. A specialization for certain applications is necessary. Measurements and statements on the data of the reflex sensors are made relative to a reference surface with defined properties and precisely known reflecting properties. This reference medium is the diffusely reflecting Kodak neutral card, also known as gray card (KODAK neutral test card; KODAK publication No. Q-13, CAT 1527654). It is also used here as the reference medium for all details. The reflection factor of the white side of the card is 90% and that of the gray side is 18%.

Table 1 shows the measured reflection of a number of materials which are important for the practical use of sensors. The values of the collector current given are relative and correspond to the reflection of the various surfaces with regard to the sensor's receiver. They were measured at a transmitter current of  $I_F = 20 \text{ mA}$  and at a distance of the maximum light coupling. These values apply to all reflex sensors. The 'black-on-white paper' section stands out in table 1. Although all surfaces appear black to the 'naked eye', the black surfaces emit quite different reflections at a wavelength of 950 nm. It is particularly important to account for this fact when using reflex sensors. The reflection of the various body surfaces in the infrared range can deviate significantly from that in the visible range.

Table 1. Relative collector current (or coupling factor) of the reflex sensors for reflection on various materials. Reference is the white side of the Kodak neutral card. The sensor is positioned perpendicular to the surface. The wavelength is 950 nm.

<b>Kodak neutral card</b>	
<b>White side (reference medium)</b>	<b>100%</b>
Gray side	20%
<b>Paper</b>	
Typewriting paper	94%
Drawing card, white (Schoeller Durex)	100%
Card, light gray	67%
Envelope (beige)	100%
Packing card (light brown)	84%
Newspaper paper	97%
Pergament paper	30-42%
<b>Black on white typewriting paper</b>	
Drawing ink (Higgins, Pelikan, Rotring)	4-6%
Foil ink (Rotring)	50%
Fiber-tip pen (Edding 400)	10%
Fiber-tip pen, black (Stabilo)	76%
Photocopy	7%
<b>Plotter pen</b>	
HP fiber-tip pen (0.3 mm)	84%
Black 24 needle printer (EPSON LQ-500)	28%
Ink (Pelikan)	100%
Pencil, HB	26%

<b>Plastics, glass</b>	
White PVC	90%
Gray PVC	11%
Blue, green, yellow, red PVC	40-80%
White polyethylene	90%
White polystyrene	120%
Gray partinax	9%
<b>Fiber glass board material</b>	
Without copper coating	12-19%
With copper coating on the reverse side	30%
Glass, 1 mm thick	9%
Plexiglass, 1 mm thick	10%
<b>Metals</b>	
Aluminum, bright	110%
Aluminum, black anodized	60%
Cast aluminum, matt	45%
Copper, matt (not oxidized)	110%
Brass, bright	160%
Gold plating, matt	150%
<b>Textiles</b>	
White cotton	110%
Black velvet	1.5%

## Parameters and Practical Use of the Reflex Sensors

A reflex sensor is used in order to receive a reflected signal from an object. This signal gives information on the position, movement, size or condition (e.g. coding) of the object in question. The parameter that describes the function of the optical coupling precisely is the so-called optical transfer function (OT) of the sensor. It is the ratio of the received to the emitted radiant power.

$$OT = \frac{\Phi_r}{\Phi_e}$$

Additional parameters of the sensor, such as operating range, the resolution of optical distance of the object, the sensitivity and the switching point in the case of local changes in the reflection, are directly related to this optical transfer function.

In the case of reflex sensors with phototransistors as receivers, the ratio  $I_c/I_F$  (the ratio of collector current  $I_c$  to the forward current  $I_F$ ) of the diode emitter is preferred to the optical transfer function. As with optocouplers,  $I_c/I_F$  is generally known as the coupling factor,  $k$ . The following approximate relationship exists between  $k$  and OT:

$$k = I_c/I_F = [(S \times B)/h] \times \Phi_r/\Phi_e$$

where  $B$  is the current amplification,  $S = I_b/\Phi_r$  (phototransistor's spectral sensitivity), and  $h = I_F/\Phi_e$  (proportionality factor between  $I_F$  and  $\Phi_e$  of the transmitter).

In figures 7 and 8, the curves of the radiant intensity,  $I_e$ , of the transmitter to the forward current,  $I_F$ , and the sensitivity of the detector to the irradiance,  $E_e$ , are shown respectively. The gradients of both are equal to unity slope.

This represents a measure of the deviation of the curves from the ideal linearity of the parameters. There is a good proportionality between  $I_e$  and  $I_F$  and between  $I_c$  and  $E_e$  where the curves are parallel to the unity gradient.

Greater proportionality improves the relationship between the coupling factor,  $k$ , and the optical transfer function.

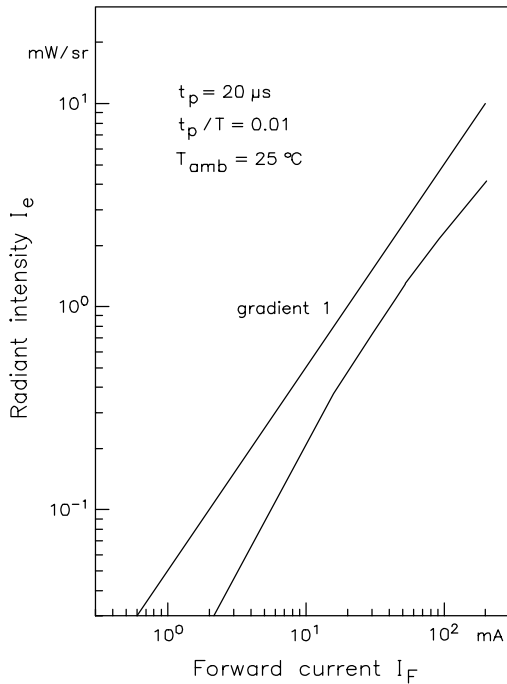


Figure 7. Radiant intensity,  $I_e = f(I_F)$ , of the IR transmitter

### Coupling Factor, $k$

In the case of reflex couplers, the specification of the coupling factor is only useful by a defined reflection and distance. Its value is given as a percentage and refers here to the diffuse reflection (90%) of the white side of Kodak neutral card at the distance of the maximum light coupling. Apart from the transmitter current,  $I_F$ , and the temperature, the coupling factor also depends on the distance from the reflecting

surface and the frequency – that is, the speed of reflection change.

For all reflex sensors, the curve of the coupling factor as a function of the transmitter current,  $I_F$ , has a flat maximum at approximately 30 mA (figure 9). As shown in the figure, the curve of the coupling factor follows that of the current amplification,  $B$ , of the phototransistor. The influence of temperature on the coupling factor is relatively small and changes approximately  $-10\%$  in the range of  $-10$  to  $+70^\circ\text{C}$  (figure 10). This fairly favorable temperature compensation is attributable to the opposing temperature coefficient of the IR diode and the phototransistor.

The maximum speed of a reflection change that is detectable by the sensor as a signal is dependent either on the switching times or the threshold frequency,  $f_c$ , of the component. The threshold frequency and the switching times of the reflex sensors TCRT1000, TCRT5000, and CNY70 are determined by the slowest component in the system – in this case the phototransistor. As usual, the threshold frequency,  $f_c$ , is defined as the frequency at which the value of the coupling factor has fallen by 3 dB (approximately 30%) of its initial value. As the frequency increases,  $f > f_c$ , the coupling factor decreases.

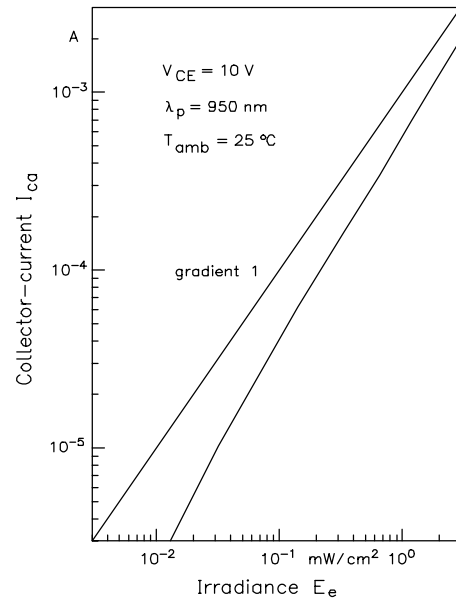


Figure 8. Sensitivity of the reflex sensors' detector

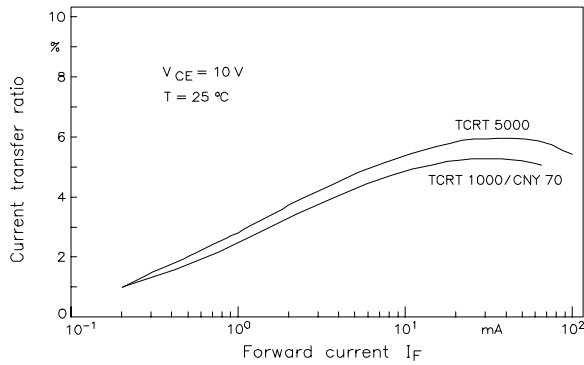


Figure 9. Coupling factor  $k = f(I_F)$  of the reflex sensors

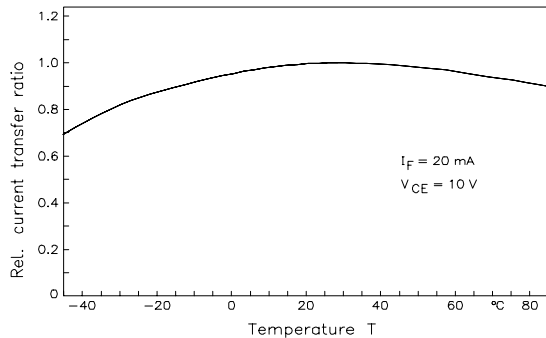


Figure 10. Change of the coupling factor,  $k$ , with temperature,  $T$

As a consequence, the reflection change is no longer easily identified.

Figure 11 illustrates the change of the cut-off frequency at collector emitter voltages of 5, 10 and 20 V and various load resistances. Higher voltages and low load resistances significantly increase the cut-off frequency.

The cut-off frequencies of all Vishay Semiconductor reflex sensors are high enough (with 30 to 50 kHz) to recognize extremely fast mechanical events.

In practice, it is not recommended to use a large load resistance to obtain a large signal, dependent on the speed of the reflection change. Instead, the opposite effect takes place, since the signal amplitude is markedly reduced by the decrease in the cut-off frequency. In practice, the better approach is to use the given data of the application (such as the type of mechanical movement or the number of markings on the reflective medium). With these given data, the maximum speed at which the reflection changes can be determined, thus allowing the maximum frequency occurring to be calculated. The maximum permissible load resistance can then be selected for this frequency

from the diagram  $f_c$  as a function of the load resistance,  $R_L$ .

### Working Diagram

The dependence of the phototransistor collector current on the distance,  $A$ , of the reflecting medium is shown in figures 12 and 13 for the reflex sensor TCRT1000.

The data were recorded for the Kodak neutral card with 90% diffuse reflection serving as the reflecting surface, arranged perpendicular to the sensor. The distance,  $A$ , was measured from the surface of the reflex sensor.

The emitter current,  $I_F$ , was held constant during the measurement. Therefore, this curve also shows the course of the coupling factor and the optical transfer function over distance. It is called the working diagram of the reflex sensor.

The working diagrams of all sensors (figure 12) shows a maximum at a certain distance,  $A_0$ . Here the optical coupling is the strongest. For larger distances, the collector current falls in accordance with the square law. When the amplitude,  $I$ , has fallen not more than 50% of its maximum value, the operation range is at its optimum.

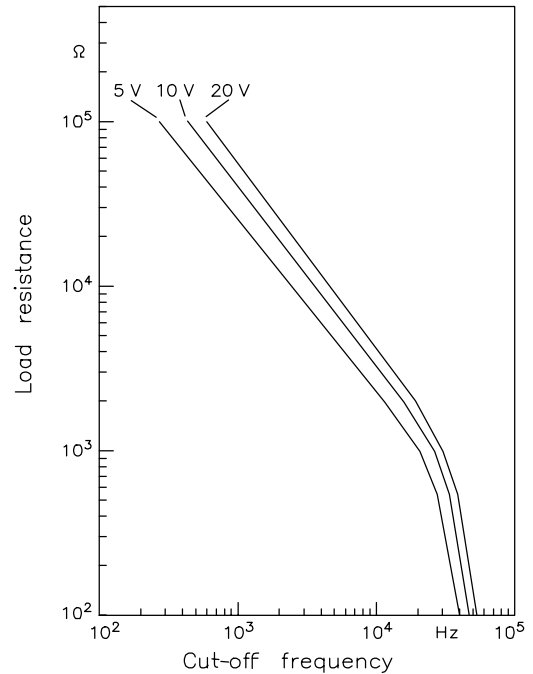
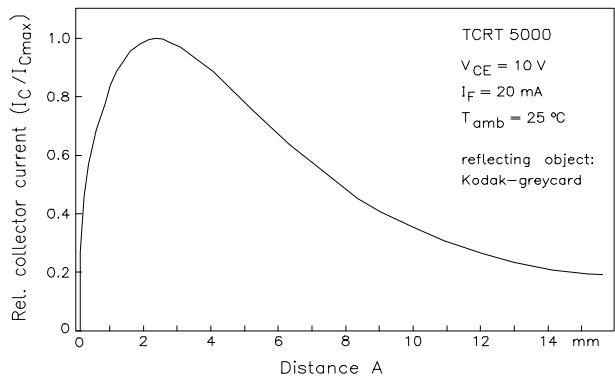
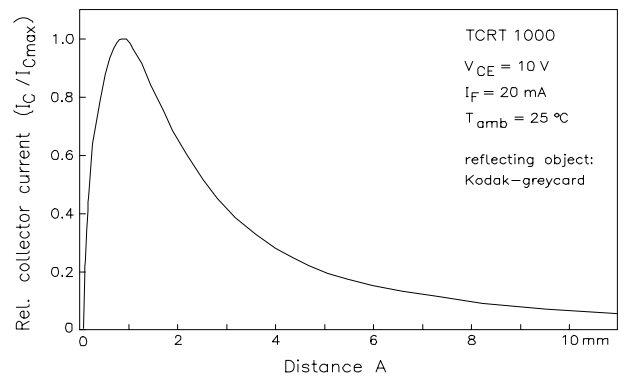


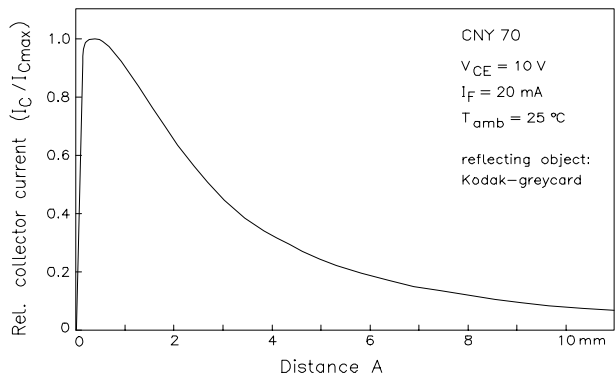
Figure 11. Cut-off frequency,  $f_c$



a) TCRT5000



c) TCRT1000



b) CNY 70

Figure 12. Working diagram of reflex sensors TCRT5000, CNY70 and TCRT1000

### Resolution, Trip Point

The behavior of the sensors with respect to abrupt changes in the reflection over a displacement path is determined by two parameters: the resolution and the trip point.

If a reflex sensor is guided over a reflecting surface with a reflection surge, the radiation reflected back to the detector changes gradually, not abruptly. This is depicted in figure 13a. The surface,  $g$ , seen jointly by the transmitter and detector, determines the radiation received by the sensor. During the movement, this surface is gradually covered by the dark reflection range. In accordance with the curve of the radiation detected, the change in collector current is not abrupt, but undergoes a wide, gradual transition from the higher to the lower value.

As illustrated in figure 13b, the collector current falls to the value  $I_{c2}$ , which corresponds to the reflection of the

dark range, not at the point  $X_0$ , but at the points  $X_0 + X_{d/2}$ , displaced by  $X_{d/2}$ .

The displacement of the signal corresponds to an uncertainty when recording the position of the reflection change, and it determines the resolution and the trip point of the sensor.

The trip point is the position at which the sensor has completely recorded the light/ dark transition, that is, the range between the points  $X_0 + X_{d/2}$  and  $X_0 - X_{d/2}$  around  $X_0$ . The displacement,  $X_d$ , therefore, corresponds to the width or the tolerance of the trip point. In practice, the section lying between 10 and 90% of the difference  $I_c = I_{c1} - I_{c2}$  is taken as  $X_d$ . This corresponds to the rise time of the generated signal since there is both movement and speed. Analogous to switching time, displacement,  $X_d$ , is described as a switching distance.

The resolution is the sensor's capability to recognize small structures. Figure 13 illustrates the example of the curve of the reflection and current signal for a black line measuring  $d$  in width on a light background (e.g. on a sheet of paper). The line has two light/ dark transitions – the switching distance  $X_{d/2}$  is, therefore, effective twice.

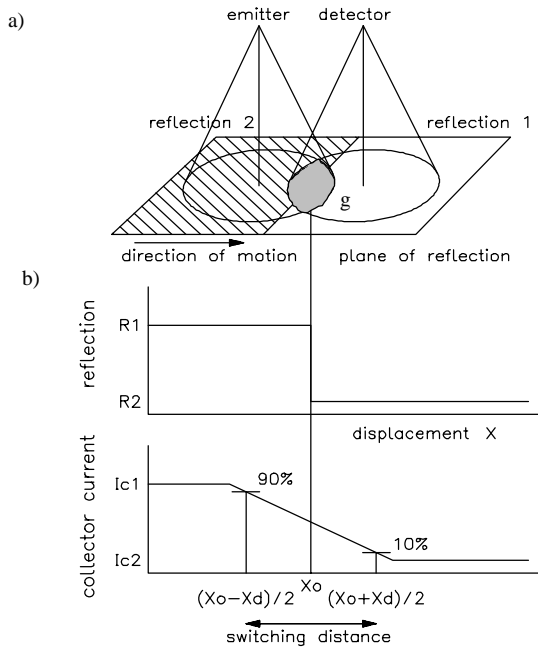


Figure 13. Abrupt reflection change with associated  $I_c$  curve

The line is clearly recognized as long as the line width is  $d \geq X_d$ . If the width is less than  $\geq X_d$ , the collector current change,  $I_{c1} - I_{c2}$ , that is the processable signal, becomes increasingly small and recognition increasingly uncertain. The switching distance – or better its inverse – can therefore be taken as a resolution of the sensor.

The switching distance,  $X_d$ , is predominantly dependent on the mechanical/ optical design of the sensor and the distance to the reflecting surface. It is also influenced by the relative position of the transmitter/ detector axis.

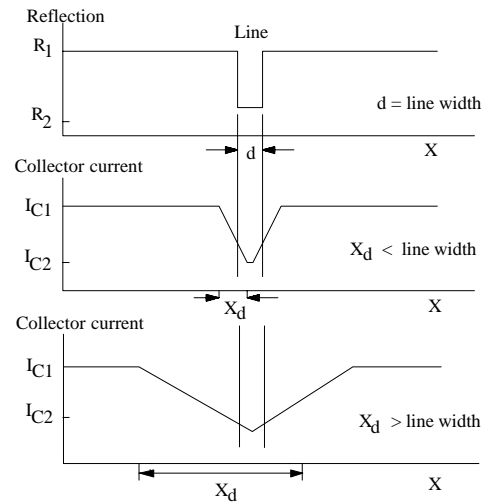


Figure 14. Reflection of a line of width  $d$  and corresponding curve of the collector current  $I_c$

Figure 14 shows the dependence of the switching distance,  $X_d$ , on the distance  $A$  with the sensors placed in two different positions with respect to the separation line of the light/ dark transition.

The curves marked position 1 in the diagrams correspond to the first position. The transmitter/ detector axis of the sensor was perpendicular to the separation line of the transition. In the second position (curve 2), the transmitter/ detector axis was parallel to the transition.

In the first position (1) all reflex sensors have a better resolution (smaller switching distances) than in position 2. It can recognize lines smaller than half a millimeter at a distance below 0.5 mm.

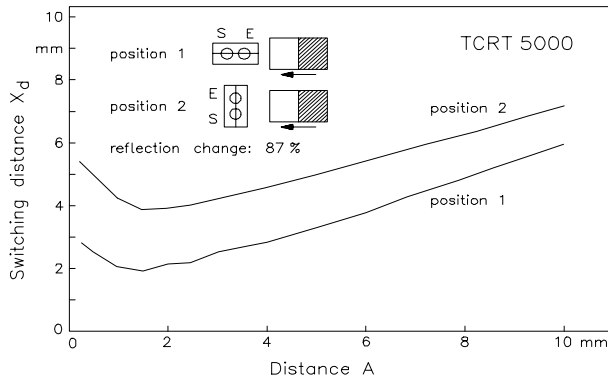
It should be remarked that the diagram of TCRT5000 is scaled up to 10 cm. It shows best resolution between 2 and 10 cm.

All sensors show the peculiarity that the maximum resolution is not at the point of maximum light coupling,  $A_0$ , but at shorter distances.

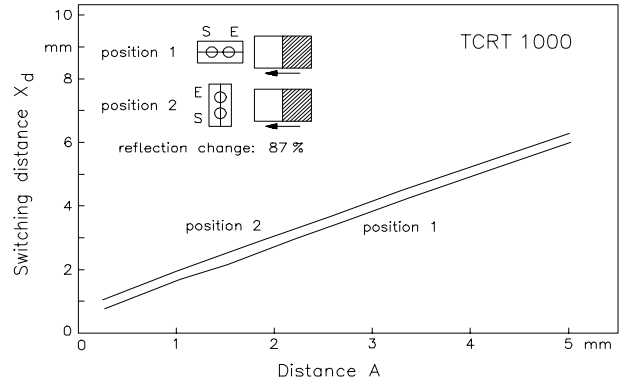
In many cases, a reflex sensor is used to detect an object that moves at a distance in front of a background, such as a sheet of paper, a band or a plate. In contrast to the examples examined above, the distances of the object surface and background from the sensor vary.

Since the radiation received by the sensor's detector depends greatly on the distance, the case may arise when the difference between the radiation reflected by the object on the background is completely equalized by the distance despite varying reflectance factors. Even if the sensor has sufficient resolution, it will no

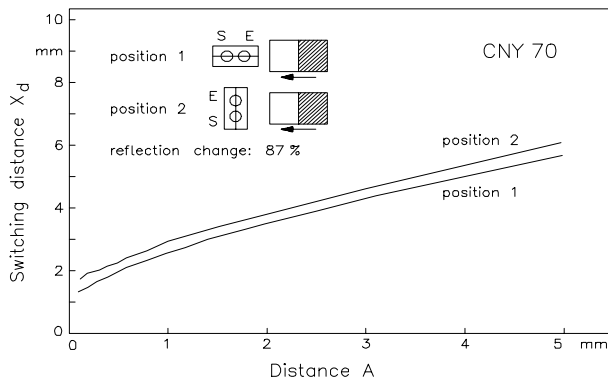
longer supply a processable signal due to the low reflection difference. In such applications it is necessary to examine whether there is a sufficient contrast. This is performed with the help of the working diagram of the sensor and the reflectance factors of the materials.



a) TCRT5000



c) TCRT1000



b) CNY70

Figure 15. The switching distance as a function of the distance A for the reflex sensors TCRT5000, CNY70 and TCRT1000



### Sensitivity, Dark Current and Crosstalk

The lowest photoelectric current that can be processed as a useful signal in the sensor's detector determines the weakest usable reflection and defines the sensitivity of the reflex sensor. This is determined by two parameters – the dark current of the phototransistor and the crosstalk.

The phototransistor as receiver exhibits a small dark current,  $I_{CEO}$ , of a few nA at 25°C. However, it is dependent on the applied collector-emitter voltage,  $V_{CE}$ , and to a much greater extent on the temperature,  $T$  (see figure 16). The crosstalk between the transmitter and detector of the reflex sensor is given with the current,  $I_{CX}$ .  $I_{CX}$  is the collector current of the photoelectric transistor measured at normal IR transmitter operating conditions without a reflecting medium.

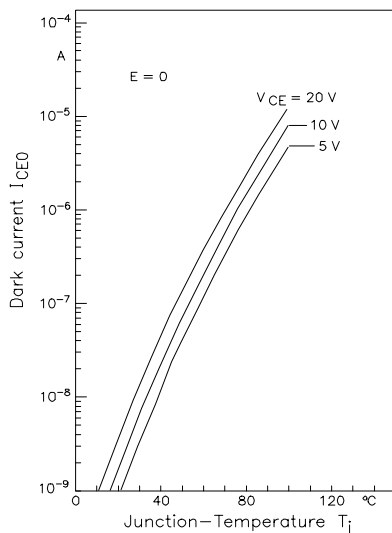


Figure 16. Temperature-dependence of the collector dark current

It is ensured that no (ambient) light falls onto the photoelectric transistor. This determines how far it is possible to guarantee avoiding a direct optical connection between the transmitter and detector of the sensor.

At  $I_F = 20$  mA, the current  $I_{CX}$  is approximately 15 nA for the CNY70, TCRT1000 and TCRT5000.

$I_{CX}$  can also be manifested dynamically. In this case, the origin of the crosstalk is electrical rather than optical.

For design and optical reasons, the transmitter and detector are mounted very close to each other.

Electrical interference signals can be generated in the detector when the transmitter is operated with a pulsed or modulated signal. The transfer capability of the interference increases strongly with the frequency. Steep pulse edges in the transmitter's current are particularly effective here since they possess a large portion of high frequencies. For all Vishay Semiconductor sensors, the ac crosstalk,  $I_{CXac}$ , does not become effective until frequencies of 4 MHz upwards with a transmission of approximately 3 dB between the transmitter and detector.

The dark current and the dc - and ac crosstalk form the overall collector fault current,  $I_{CF}$ . It must be observed that the dc-crosstalk current,  $I_{CXdc}$ , also contains the dark current,  $I_{CEO}$ , of the phototransistor.

$$I_{CF} = I_{CXdc} + I_{CXac}$$

This current determines the sensitivity of the reflex sensor. The collector current caused by a reflection change should always be at least twice as high as the fault current so that a processable signal can be reliably identified by the sensor.

### Ambient Light

Ambient light is another feature that can impair the sensitivity and, in some circumstances, the entire function of the reflex sensor. However, this is not an artifact of the component, but an application specific characteristic.

The effect of ambient light falling directly on the detector is always very troublesome. Weak steady light reduces the sensor's sensitivity. Strong steady light can, depending on the dimensioning ( $R_L$ ,  $V_C$ ), saturate the photoelectric transistor. The sensor is 'blind' in this condition. It can no longer recognize any reflection change. Chopped ambient light gives rise to incorrect signals and feigns non-existent reflection changes.

Indirect ambient light, that is ambient light falling onto the reflecting objects, mainly reduces the contrast between the object and background or the feature and surroundings. The interference caused by ambient light is predominantly determined by the various reflection properties of the material which in turn are dependent on the wavelength.



If the ambient light has wavelengths for which the ratio of the reflection factors of the object and background is the same or similar, its influence on the sensor's function is small. Its effect can be ignored for intensities that are not excessively large. On the other hand, the object/ background reflection factors can differ from each other in such a way that, for example, the background reflects the ambient light much more than the object. In this case, the contrast disappears and the object cannot be detected. It is also possible that an uninteresting object or feature is detected by the sensor because it reflects the ambient light much more than its surroundings.

In practice, ambient light stems most frequently from filament, fluorescent or energysaving lamps. Table 2 gives a few approximate values of the irradiance of these sources. The values apply to a distance of approximately 50 cm, the spectral range to a distance of 850 to 1050 nm. The values of table 2 are only intended as guidelines for estimating the expected ambient radiation.

In practical applications, it is generally rather difficult to

determine the ambient light and its effects precisely. Therefore, an attempt to keep its influence to a minimum is made from the outset by using a suitable mechanical design and optical filters. The detectors of the sensors are equipped with optical filters to block such visible light. Furthermore, the mechanical design of these components is such that it is not possible for ambient light to fall directly or sideways onto the detector for object distances of up to 2 mm.

If the ambient light source is known and is relatively weak, in most cases it is enough to estimate the expected power of this light on the irradiated area and to consider the result when dimensioning the circuit.

AC operation of the reflex sensors offers the most effective protection against ambient light. Pulsed operation is also helpful in some cases.

Compared with dc operation, the advantages are greater transmitter power and at the same time significantly greater protection against faults. The only disadvantage is the greater circuit complexity, which is necessary in this case. The circuit in figure 20 is an example of operation with chopped light.

Table 2. Examples for the irradiance of ambient light sources

Light source (at 50 cm distance)	Irradiance $E_e$ ( $\mu\text{W}/\text{cm}^2$ ) 850 to 1050 nm		Frequency (Hz)
	Steady light	AC light (peak value)	
Filament lamp (60 W)	500		
Fluorescent lamp OSRAM (65 W)	25	30	100
Economy lamp OSRAM DULUX (11 W)	14	16	100

## Application Examples, Circuits

The most important characteristics of the Vishay Semiconductor reflex sensors are summarized in table 3. The task of this table is to give a quick comparison of data for choosing the right sensor for a given application.

### Application Example with Dimensioning

With a simple application example, the dimensioning of the reflex sensor can be shown in the basic circuit with the aid of the component data and considering the boundary conditions of the application.

The reflex sensor is used for speed control. An aluminum disk with radial strips as markings fitted to the motor shaft forms the reflecting object and is located approximately 3 mm in front of the sensor. The sensor signal is sent to a logic gate for further processing.

Dimensioning is based on dc operation, due to the simplified circuitry.

The optimum transmitter current,  $I_F$  for dc operation is between 20 and 40 mA.  $I_F = 20$  mA is selected in this case.

As shown in figure 17, the coupling factor is at its maximum. In addition, the degradation (i.e. the reduction of the transmitted IR output with aging) is minimum for currents under 40 mA (< 10% for 10000 h) and the self heating is low due to the power loss (approximately 50 mW at 40 mA).

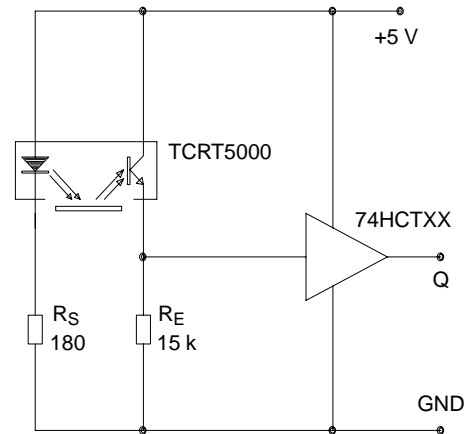


Figure 17. Reflex sensor - basic circuit

Table 3.

Parameter	Symbol	Reflex Sensor Type		
		CNY70	TCRT1000	TCRT5000
Distance of optimum coupling	$A_0$	0.3 mm	1 mm	2 mm
Distance of best resolution	$A_r$	0.2 mm	0.8 mm	1.5 mm
Coupling factor	$k$	5%	5%	6%
Switching distance (min.)	$x_d$	1.5 mm	0.7 mm	1.9 mm
Optimum working distance	$X_{or}$	0.2 to 3 mm	0.4 to 2.2 mm	0.2 to 6.5 mm
Operating range	$A_{or}$	9 mm	8 mm	> 20 mm

Table 4.

Application Data	
Aluminum disk	Diameter 50 mm, distance from the sensor 3 mm, markings printed on the aluminum
Markings	8 radial black stripes and 8 spacings, the width of the stripes and spacings in front of the sensor is approximately = 4 mm (in a diameter of 20 mm)
Motor speed	1000 to 3000 rpm
Temperature range	10 to 60°C
Ambient light	60 W fluorescent lamp, approximate distance 2 m
Power supply	5 V ± 5%
Position of the sensor	Position 1, sensor/ detector connecting line perpendicular to the strips

Special attention must also be made to the downstream logic gate. Only components with a low input offset current may be used. In the case of the TTL gate and the LS-TTL gate, the  $I_{LH}$  current can be applied to the sensor output in the low condition. At  $-1.6$  mA or  $-400$   $\mu$ A, this is above the signal current of the sensor. A transistor or an operational amplifier should be connected at the output of the sensor when TTL or LS-TTL components are used. A gate from the 74HCTxx family is used.

According to the data sheet, its fault current  $I_{LH}$  is approximately 1  $\mu$ A.

The expected collector current for the minimum and maximum reflection is now estimated.

According to the working diagram in figure 12a, it follows that when  $A = 3$  mm

$$I_c = 0.95 \times I_{cmax}$$

$I_{cmax}$  is determined from the coupling factor,  $k$ , for  $I_F = 10$  mA.

$$I_{cmax} = k \times I_F$$

At  $I_F = 10$  mA, the typical value

$$k = 2.8\%$$

is obtained for  $k$  from figure 9.

However, this value applies to the Kodak neutral card or the reference surface. The coupling factor has a different value for the surfaces used (typewriting paper and black-fiber tip pen). The valid value for these material surfaces can be found in table 1:

$$k_1 = 94\% \times k = 4.7\% \text{ for typing paper and}$$

$$k_2 = 10\% \times k = 0.5\% \text{ for black-tip pen (Edding)}$$

$$\text{Therefore: } I_{c1} = 0.95 \times k_1 \times I_F = 446.5 \mu\text{A}$$

$$I_{c2} = 0.95 \times k_2 \times I_F = 47.5 \mu\text{A}$$

Temperature and aging reduce the collector current. They are therefore important to  $I_{c1}$  and are subtracted from it.

Figure 10 shows a change in the collector current of approximately 10% for 70°C. Another 10% is deducted from  $I_{c1}$  for aging

$$I_{c1} = 263 \mu\text{A} - (20\% \times 263 \mu\text{A}) = 357.2 \mu\text{A}$$

The fault current  $I_{cf}$  (from crosstalk and collector dark current) increases the signal current and is added to

$I_{c2}$ . Crosstalk with only a few nA for the TCRT5000 is ignored. However, the dark current can increase up to 1  $\mu$ A at a temperature of 70°C and should be taken into account.

In addition, 1  $\mu$ A, the fault current of the 74HCTxx gate, is also added

$$I_{c2} = 49.5 \mu\text{A}$$

The effect of the indirect incident ambient light can most easily be seen by comparing the radiant powers produced by the ambient light and the sensor's transmitter on 1 mm<sup>2</sup> of the reflecting surface. The ambient light is then taken into account as a percentage in accordance with the ratio of the powers.

From table 2:

$$E_e(0.5 \text{ m}) = 40 \mu\text{W}/\text{cm}^2 \text{ (dc + ac/ 2)}$$

$$E_e(2 \text{ m}) = E_e(0.5 \text{ m}) \times (0.5/ 2)^2$$

(Square of the distance law)

$$E_e(2 \text{ m}) = 2.5 \mu\text{W}/\text{cm}^2$$

$$\Phi_{sf} = 0.025 \mu\text{W}$$

The radiant power ( $\Phi_{sf} = 0.025 \mu\text{W}$ ) therefore falls on 1 mm<sup>2</sup>.

When  $I_F = 10$  mA, the sensor's transmitter has the radiant intensity:

$$I_e = \frac{\Phi_e}{\Omega} = 0.25 \text{ W/sr}$$

(see figure 7)

The solid angle for 1 mm<sup>2</sup> surface at a distance of 3 mm is

$$\Omega = \frac{1 \text{ mm}^2}{(3 \text{ mm})^2} = \frac{1}{9} \text{ sr}$$

It therefore follows for the radiant power that:

$$\Phi_e = I_e \times \Omega = \text{ca. } 27.8 \text{ mW}$$

The power of 0.025  $\mu$ W produced by the ambient light is therefore negligibly low compared with the corresponding power (approximately 28  $\mu$ W) of the transmitter.

The currents  $I_{c1}$ ,  $I_{c2}$  would result in full reflecting surfaces, that is, if the sensor's visual field only measures white or black typing paper. However, this is not the case. The reflecting surfaces exist in the form of stripes.

The signal can be markedly reduced by the limited resolution of the sensor if the stripes are narrow. The suitable stripe width for a given distance should therefore be selected from figure 15. In this case, the minimum permissible stripe width is approximately 2.5 mm for a distance of 3 mm (position 1, figure 15a). The markings measuring 4 mm in width were expediently selected in this case. For this width, a signal reduction of about 20% can be permitted with relatively great certainty, so that 10% of the difference ( $I_{c1} - I_{c2}$ ) can be subtracted from  $I_{c1}$  and added to  $I_{c2}$ .

$$I_{c1} = 357.2 \mu\text{A} - 30.8 \mu\text{A} = 326.4 \mu\text{A}$$

$$I_{c2} = 49.5 \mu\text{A} + 30.8 \mu\text{A} = 80.3 \mu\text{A}$$

The suitable load resistance,  $R_E$ , at the emitter of the photo-transistor is then determined from the low and high levels 0.8 V and 2.0 V for the 74HCTxx gate.

$$R_E < 0.8 \text{ V} / I_{c2} \text{ and } R_E > 2.0 \text{ V} / I_{c1},$$

i.e.,  $6.1 \text{ k}\Omega < R_E < 9.96 \text{ k}\Omega$   
 6.8 kΩ is selected for  $R_E$

The corresponding levels for determining  $R_E$  must be used if a Schmitt trigger of the 74HCTxx family is employed.

The frequency limit of the reflex sensor is then determined with  $R_E = 6.8 \text{ k}\Omega$  and compared with the maximum operating frequency in order to check whether signal damping attributable to the frequency can occur.

Figure 11 shows for  $V_s = 5 \text{ V}$  and  $R_E = 6.8 \text{ k}\Omega$  approximately, for the TCRT5000,  $f_c = 3.0 \text{ kHz}$ .

Sixteen black/ white stripes appear in front of the sensor in each revolution. This produces a maximum signal frequency of approximately 400 Hz for the maximum speed of 3000 rpm up to 50 rps. This is significantly less than the  $f_c$  of the sensor, which means there is no risk of signal damping.

In the circuit in figure 17, a resistor,  $R_C$ , can be used on the collector of the photoelectric transistor instead of  $R_E$ . In this case, an inverted signal and somewhat modified dimensioning results. The current  $I_{c1}$  now determines the low signal level and the current  $I_{c2}$  the high. The voltages ( $V_s - 2 \text{ V}$ ) and ( $V_s - 0.8 \text{ V}$ ) and not the high level and low level 2 V and 0.8 V, are now decisive for determining the resistance,  $R_C$ .

### Circuits with Reflex Sensors

The couple factor of the reflex sensors is relatively small. Even in the case of good reflecting surfaces, it is less than 10%. Therefore, the photocurrents are in practice only in the region of a few  $\mu\text{A}$ . As this is not enough to process the signals any further, an additional amplifier is necessary at the sensor output.

Figure 18 shows two simple circuits with sensors and follow-up operational amplifiers.

The circuit in figure 18b is a transimpedance which offers in addition to the amplification the advantage of a higher cut-off frequency for the whole layout.

Two similar amplification circuits incorporating transistors are shown in figure 19.

The circuit in figure 20 is a simple example for operating the reflex sensors with chopped light. It uses a pulse generator constructed with a timer IC. This pulse generator operates with the pulse duty factor of approximately 1. The frequency is set to approximately 22 kHz. On the receiver side, a conventional LC resonance circuit ( $f_o = 22 \text{ kHz}$ ) filters the fundamental wave out of the received pulses and delivers it to an operational amplifier via the capacitor,  $C_k$ . The LC resonance circuit simultaneously represents the photo transistor's load resistance. For direct current, the photo transistor's load resistance is very low – in this case approximately 0.4, which means that the photo transistor is practically shorted for dc ambient light.

At resonance frequencies below 5 kHz, the necessary coils and capacitors for the oscillator become unwieldy and expensive. Therefore, active filters, made up with operational amplifiers or transistors, are more suitable (figures 21 and 22). It is not possible to obtain the quality characteristics of passive filters. In addition the load resistance on the emitter of the photo transistor has remarkably higher values than the dc resistance of a coil. On the other hand, the construction with active filters is more compact and cheaper. The smaller the resonance frequency becomes, the greater the advantages of active filters compared to LC resonant circuits.

In some cases, reflex sensors are used to count steps or objects, while at the same time recognition of a change in the direction of rotation (= movement direction) is necessary. The circuit shown in figure 23 is suitable for such applications. The circuit is composed of two independent channels with reflex sensors. The sensor signals are formed via the Schmitt trigger into TTL impulses with step slopes, which are supplied to the pulse inputs of the binary counter 74LS393. The outputs of the 74LS393 are coupled to the reset inputs. This is made in such a way that the first output, whose condition changes from 'low' to 'high', sets the directly connected counter. In this way, the counter of the other channel is deleted and blocked. The outputs of the active counter can be displaced or connected to more electronics for evaluation.

It should be mentioned that such a circuit is only suited to evenly distributed objects and constant movements. If this is not the case, the channels must be close to each other, so that the movement of both sensors are collected successively. The circuit also works perfectly if the last mentioned condition is fulfilled. Figure 24 shows a pulse circuit combining analog with digital components and offering the possibility of temporary storage of the signal delivered by the reflex sensor. A timer IC is used as the pulse generator.

The negative pulse at the timer's output triggers the clock input of the 74HCT74 flip-flop and, at the same

time, the reflex sensor's transmitter via a driver transistor. The flip-flop can be positively triggered, so that the condition of the data input at this point can be received as the edge of the pulse rises. This then remains stored until the next rising edge.

The reflex sensor is therefore only active for the duration of the negative pulse and can only detect reflection changes within this time period. During the time of negative impulses, electrical and optical interferences are suppressed. A sample and hold circuit can also be employed instead of the flip-flop. This is switched on via an analog switch at the sensor output as the pulse rises.

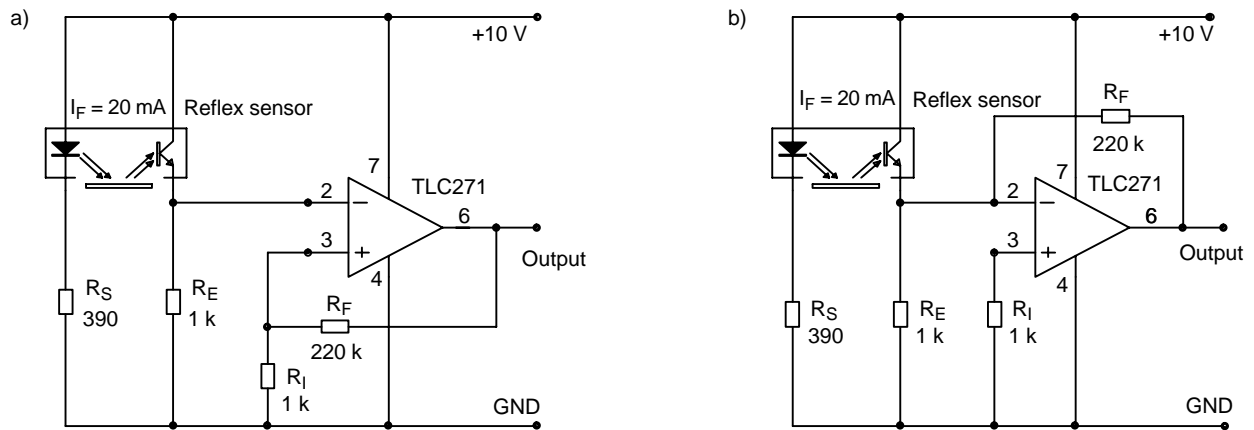


Figure 18. Circuits with operational amplifier

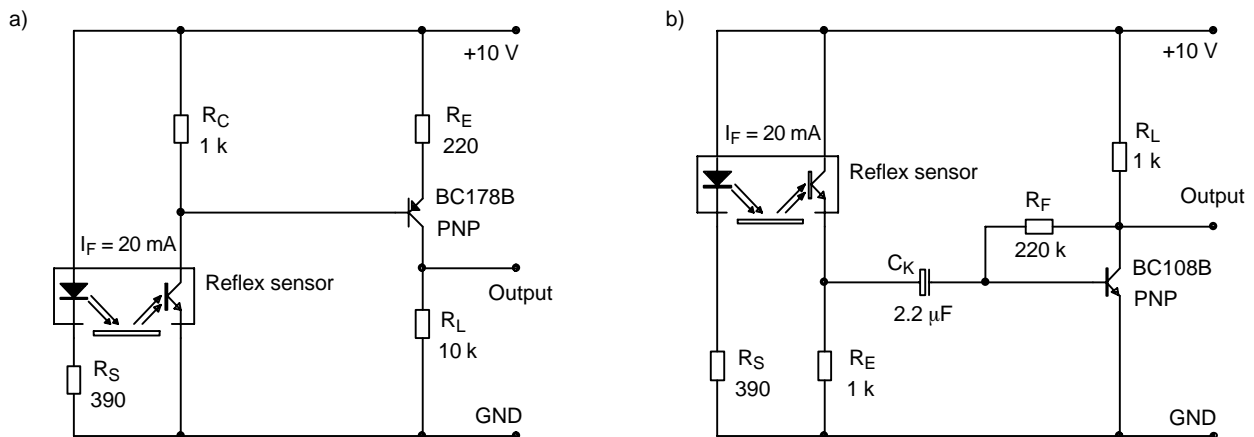


Figure 19. Circuits with transistor amplifier

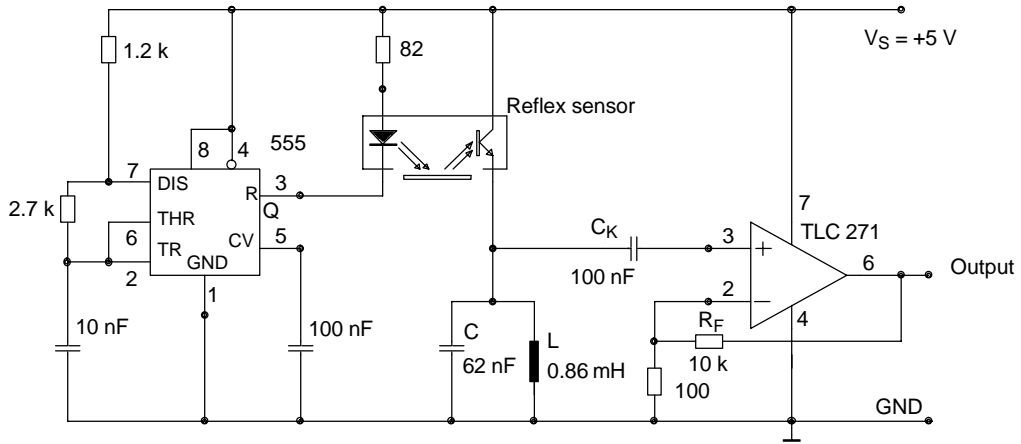
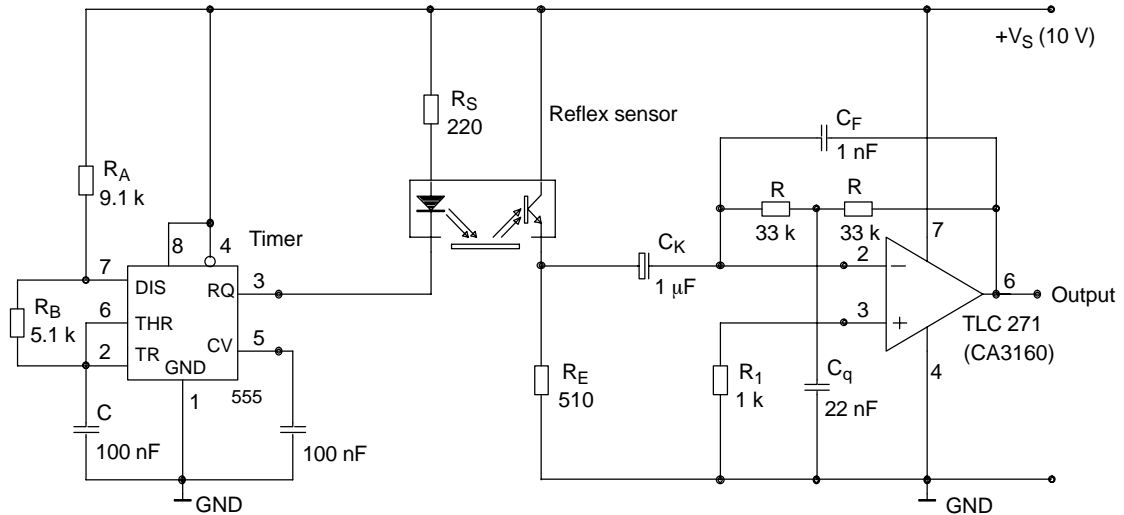


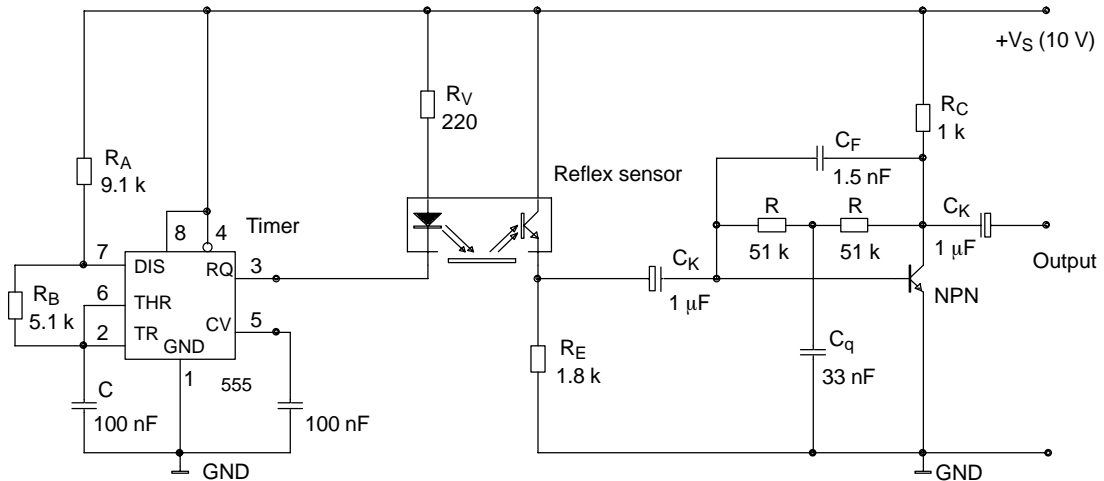
Figure 20. AC operation with oscillating circuit to suppress ambient light



Timer dimensions:  $t_p$  (pulse width) =  $0.8 RC = 400 \mu s$   
 $T$  (period) =  $0.8 (R_A + R_B) \times C = 1 ms$

Active filter:  $C = \sqrt{C_f \times C_q}$   $Q = \sqrt{\frac{C_q}{C_f}}$   
 $f_o = 1/(6.28 \times C \times R)$   $V_{uo} = \frac{2R}{R_E} \times Q^2$

Figure 21. AC operation with active filter made up of an operational amplifier, circuit and dimensions



Timer dimensions:  $t_p$  (pulse width) =  $0.8 RC = 400$  ms  
 $T$  (period) =  $0.8 (R_A + R_B) \times C = 1$  ms

Active filter :  $C = \sqrt{C_f \times C_q}$   $Q = \sqrt{\frac{C_q}{C_f}}$   
 $f_o = 1/(6.28 \times C \times R)$   $V_{uo} = \frac{2R}{R_E} \times Q^2$

Figure 22. AC operation with transistor amplifier as active filter

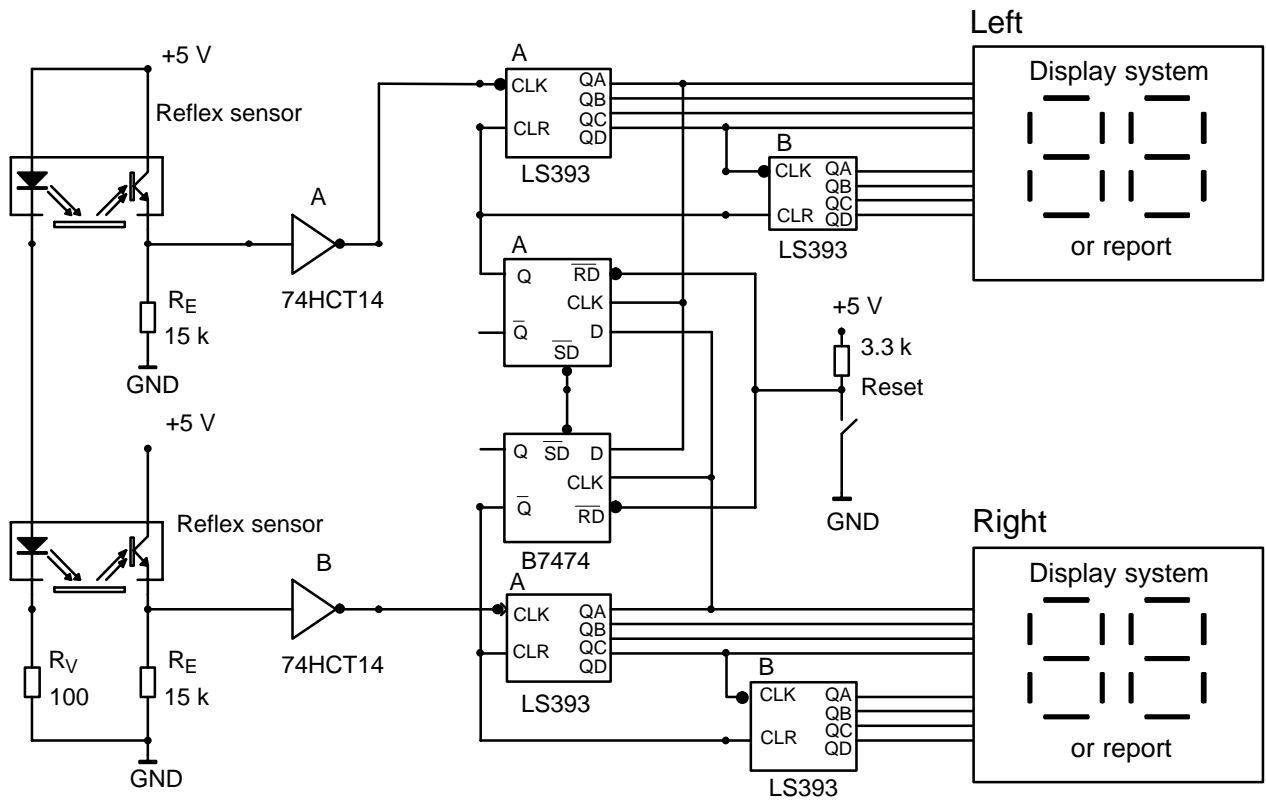


Figure 23. Circuit for objects count and recognition of movement direction



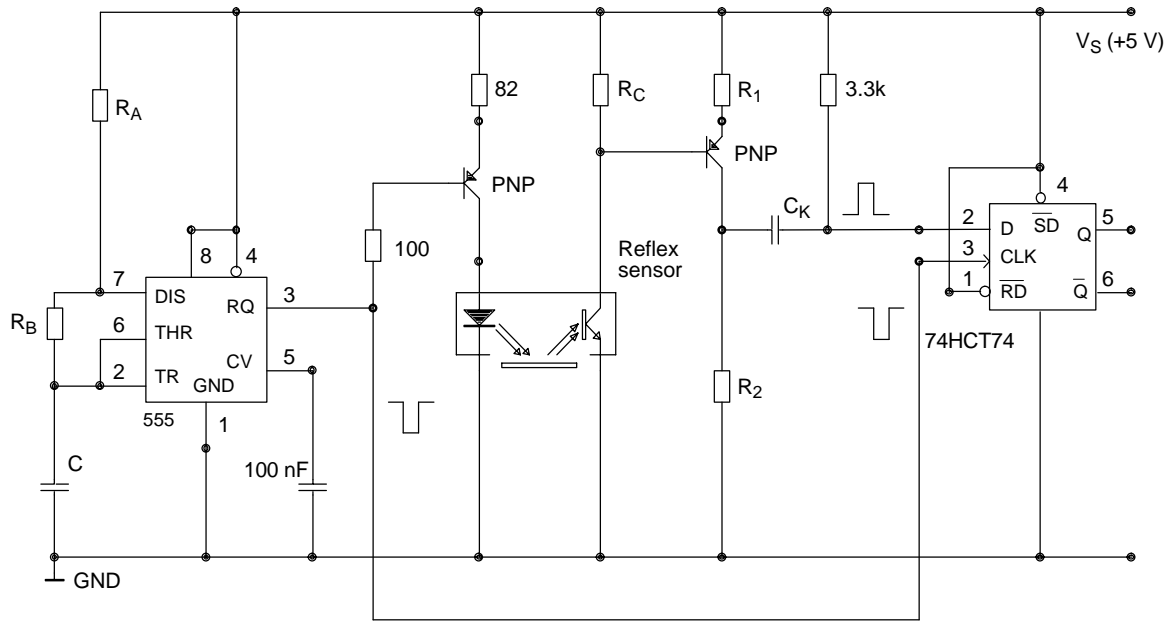


Figure 24. Pulse circuit with buffer storage